

## Article

# Approximate Analytical Solutions to Nonlinear Oscillations of Horizontally Supported Jeffcott Rotor

Vasile Marinca<sup>1,2,\*</sup> and Nicolae Herisanu<sup>1,2</sup>

<sup>1</sup> Department of Mechanics and Strength of Materials, University Politehnica Timisoara, 300222 Timisoara, Romania; nicolae.herisanu@upt.ro

<sup>2</sup> Center for Fundamental Technical Research, Romanian Academy-Branch of Timisoara, 300223 Timisoara, Romania

\* Correspondence: vmarinca@mec.upt.ro

**Abstract:** The present paper focuses on nonlinear oscillations of a horizontally supported Jeffcott rotor. An approximate solution to the system of governing equations having quadratic and cubic nonlinearities is obtained in two cases of practical interest: simultaneous and internal resonance. The Optimal Auxiliary Functions Method is employed in this study, and each governing differential equation is reduced to two linear differential equations using the so-called auxiliary functions involving a moderate number of convergence-control parameters. Explicit analytical solutions are obtained for the first time in the literature for the considered practical cases. Numerical validations proved the high accuracy of the proposed analytical solutions, which may be used further in the study of stability and in the design process of some highly performant devices.

**Keywords:** nonlinear oscillations; rotor dynamics; asymmetric nonlinearity; simultaneous and internal resonance; optimal auxiliary functions method



**Citation:** Marinca, V.; Herisanu, N. Approximate Analytical Solutions to Nonlinear Oscillations of Horizontally Supported Jeffcott Rotor. *Energies* **2022**, *15*, 1122. <https://doi.org/10.3390/en15031122>

Academic Editor: Sérgio Cruz

Received: 27 December 2021

Accepted: 28 January 2022

Published: 3 February 2022

**Publisher's Note:** MDPI stays neutral with regard to jurisdictional claims in published maps and institutional affiliations.



**Copyright:** © 2022 by the authors. Licensee MDPI, Basel, Switzerland. This article is an open access article distributed under the terms and conditions of the Creative Commons Attribution (CC BY) license (<https://creativecommons.org/licenses/by/4.0/>).

## 1. Introduction

The nonlinear dynamics of rotors have long attracted attention, being an interesting subject with considerable technical depths and breadths. The theory of oscillations was intensively developed in the field of high-speed machinery and can be used particularly in studies of a disk on a massless shaft; power generation; land, sea, and air transportation; aerospace; textiles; home appliances; or various military systems. For an analysis of simple machinery, one has to take into consideration the accurate forms of excitation, heating and supports, the complicated geometry of the rotor, and so on. There are many types of rotating machines, with different rotor sizes, complexities, speeds, loads, powers, and rigidities [1].

The nonlinear oscillations of rotating machines were studied by many researchers. Muszynska [2] proposed many possible responses of rotor–stator systems. Karlberg and Aidanpää [3] considered the nonlinear vibrations of a rotor system with clearance, analyzing the two-degree-of-freedom unbalanced shaft in relation to a non-rotating massless housing. The rotor start-up lateral vibration signal is investigated by Patel and Darpe [4]. Vibration responses are simulated for the Jeffcott rotor having two lateral degrees of freedom. The Hilbert–Huang transform is applied to investigate the coast-up rub signal, and the wavelet transform is employed for comparison purposes.

The chaotic vibration analysis of a disk–shaft system with rub impact was performed by Khanlo et al. [5], including a consideration of the Coriolis and centrifugal effect. Yabuno et al. [6] explored nonlinear normal modes which considered the natural frequencies in vertical and horizontal directions, investigating the characteristics with primary resonance. Theoretical and experimental investigations are presented by Lahriri et al. [7], considering the impact motion of the rotor against a conventional annular backing guide, and an unconventional annular guide built with four adjustable pins. Various analytical

methods, such as those proposed by Dunkerly, Stodola, and Reynolds, etc., are presented by Dimarogonas et al. [8] for the study of nonlinear dynamics.

The behavior of a non-smooth Jeffcott rotor with bearing clearance is investigated by Chavez and Wiercigroh [9], including a bifurcation analysis of the rotor system performed using TC-HAT, a toolbox of AUTO97 which proves to be useful in detecting bifurcation in non-smooth dynamical systems. Gu and Chu [10] presented an investigation of the rotor shaft in the presence of universal temperature gradients. The thermal vibration of the rotor structure is analytically modeled and investigated.

Vibration phenomena caused by aircraft hovering flight in a rub-impact rotor system is investigated by Hou et al. [11] by using bifurcation diagrams and corresponding Lyapunov exponent spectrums. Ma et al. [12] developed a model of the rotor-blade system, considering the coupling action of some factors, which include the motion of bending and torsion, the gyroscopic effects of the rotor, centrifugal stiffening, spin softening, and Coriolis force. Stochastic bifurcation, and the chaos of rub-impact rotor systems having random stiffness and excitation, are explored in reference [13]. The passive control of a rotor instability called helicopter ground resonance is studied by Bergeot et al. [14]. The passive device relies on a set of cubic nonlinear absorbers called nonlinear energy sinks, each one positioned on a blade. The model is presented and transformed to a time-invariant system by means of Fourier transform.

The nonlinear vibrations of a horizontally supported Jeffcott rotor near the resonant speed are investigated by Saeed and Gohary [15]. The multiple scales perturbation method is utilized and bifurcation analyses are conducted. The stability is investigated by using Lyapunov's first method. The modal characteristic of a rubbing rotor system with additional constraints is analyzed by Hong et al. [16]. The governing equations are obtained and the eigen problem is analyzed using the complex nonlinear mode concept.

The nonlinear vibrations of the rotor working in a magnetic field in the presence of geometric and inertia nonlinearity are analyzed by Eftekari et al. [17]. The first three vibration modes are considered, emphasizing the effects of the electromagnetic load generated by asymmetric magnetic flux density.

Li et al. [18] studied the nonlinear vibrations of a rotor system, considering cogging and harmonic effects. Governing equations are established and the effects of stator structure parameters are investigated. An efficient simulation of the misaligned multi-degree-of-freedom rotor model, which is developed to predict the transient dynamic behavior of driveshaft deflection, is introduced by Tehomeni and Alugomgo [19]. The model accounts for tight clearance as a function of contact deformation, according to the nonlinear Hertzian contact theory. Jin et al. [20] examined the nonlinear vibration characteristics of a dual-rotor aero-engine displaying blade-casing rubbing, based on numerical simulations and experimental measurements. The dynamic model is considered based on the finite element method, considering coupling misalignment, blade-casing rubbing, and nonlinearities supporting rolling element bearings. Saeed et al. [21] analyzed the dynamical characteristics of a horizontally supported asymmetric nonlinear rotor system, which is governed by two coupled second-order nonlinear differential equations with quadratic and cubic nonlinearities. In consequence, the equations of motion were analyzed in two stages and the model is studied by means of perturbation analysis, bifurcation diagrams, Poincare maps, and a frequency spectrum.

The objective of this article is to apply a new and accurate approach to nonlinear differential equations governing the oscillations of a horizontally supported Jeffcott rotor, namely the Optimal Auxiliary Functions Method (OAFM).

The OAFM is used in the present study to obtain a first-order approximate analytical solution to governing nonlinear equations with quadratic and cubic nonlinearities in two cases: simultaneous and internal resonance. Our analytical technique is effective, explicit, accurate, and proves a rapid convergence to the exact solution after the first iteration. It provides a rigorous way to control and adjust the convergence of an analytical-approximate solution by means of a moderate number of convergence-control parameters. Our technique

does not imply the presence of a small or large parameter in the governing equations, or the boundary/initial conditions, and can be applied to a variety of engineering domains. The validity of this original method is proved by comparing the results with numerical integration results. We deal with the OAFM in a proper manner and completely differently in comparison with other known techniques. The cornerstone of the validity and flexibility of this approach is in the choice of linear operators and optimal auxiliary functions, which both contribute to obtaining highly accurate results. The convergence-control parameters involved in our procedure are optimally identified in a rigorous mathematical way. Each nonlinear differential equation is reduced to two linear differential equations that do not depend on all terms of the nonlinear equation.

The present study provides accurate explicit analytical solutions which may be used further in the study of stability, and in the design process of some highly performant devices.

## 2. The Governing Equations of Motion

In this research, we consider the horizontally supported Jeffcott rotor presented in Figure 1.

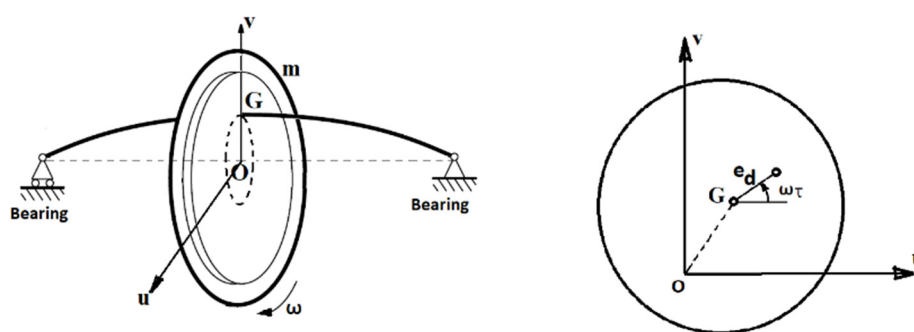


Figure 1. Jeffcott rotor system and coordinate system.

The origin  $O$  of the inertial coordinate system,  $Ouvz$ , is the intersection of the disk and the bearing center line. The whirling motion is assumed to occur on the  $U$ - $V$  plane. The mass of the disk is  $m$ , its center of gravity  $G(u,v)$  deviates slightly from the geometric center with eccentricity  $e_d$ . If  $\omega$  is the angular velocity of the rotor spinning, the restoring force  $F$  can be a symmetric nonlinear cubic function with respect to the vertical deflection  $r$  of the shaft:

$$F(r) = k_1 r + k_3 r^3 \quad (1)$$

where  $k_1$  and  $k_3$  are positive constants. The nonlinear differential equations that describe the horizontal and vertical oscillations of horizontally supported Jeffcott rotor system are expressed as follows [6,15]:

$$m\ddot{u} + c_u \dot{u} + k_1 u + k_3 u(u^2 + v^2) = me_d \omega^2 \cos \omega t \quad (2)$$

$$m\ddot{v} + c_v \dot{v} + k_1 v + k_3 v(u^2 + v^2) = me_d \omega^2 \sin \omega t - mg \quad (3)$$

where  $k_3 u(u^2 + v^2)$  and  $k_3 v(u^2 + v^2)$  is a nonlinear restoring force due to the bearing clearance,  $c_u$  and  $c_v$  are the damping coefficients in the  $U$  and  $V$  directions,  $g$  is the gravity acceleration, and the dot represents the derivative with respect to time.

From Equation (3), the deflection of the shaft due to the gravity in the static equilibrium state satisfies:

$$u(0) = 0, \quad k_1 v_{st} + k_3 v_{st}^3 = -mg \quad (4)$$

where  $v_{st}$  is the static displacement of the geometric center  $G$  due to the disk weight.

From Equation (4) it holds that:

$$v_{st} = \left[ \left( \frac{m^2 g^2}{4k_3^2} + \frac{k_1^3}{27k_3^2} \right)^{1/2} - \frac{mg}{2k_3} \right]^{1/3} - \left[ \left( \frac{m^2 g^2}{4k_3^2} + \frac{k_1^3}{27k_3^2} \right)^{1/2} + \frac{mg}{2k_3} \right]^{1/3} \tag{5}$$

as a consequence, the motion of geometrical center G in terms of deviations  $u_d$  and  $v_d$  from the static equilibrium can be rewritten in the directions U- and V- as:

$$u = 0 + u_d, v = v_{st} + v_d \tag{6}$$

and therefore, the resulting equations are:

$$m\ddot{u}_d + c_u \dot{u}_d + (k_1 + k_3 v_{st}^2)u_d + 2k_3 v_{st} u_d v_d + k_3 (u_d^2 + v_d^2)u_d = m e_d \omega^2 \cos \omega t \tag{7}$$

$$m\ddot{v}_d + c_v \dot{v}_d + (k_1 + 3k_3 v_{st}^2)v_d + k_3 v_{st} (u_d^2 + 3v_d^2) + k_3 (u_d^2 + v_d^2)v_d = m e_d \omega^2 \sin \omega t \tag{8}$$

introducing the dimensionless parameters:

$$\tau = \sqrt{\frac{k_1}{m}} t, u = \frac{u_d}{v_{st}}, v = \frac{v_d}{v_{st}} \tag{9}$$

one can get the dimensionless nonlinear differential equations of motion:

$$u'' + 2\mu_1 u' + \omega_1^2 u + 2\lambda v u + \lambda (u^3 + u v^2) = f \Omega^2 \cos \Omega \tau \tag{10}$$

$$v'' + 2\mu_2 v' + \omega_2^2 v + \lambda (u^2 + 3v^2) + \lambda (u^2 v + v^3) = f \Omega^2 \sin \Omega \tau \tag{11}$$

where the prime denotes the derivative with respect to  $\tau$ , and:

$$2\mu_1 = \frac{c_u}{\sqrt{mk_1}}; 2\mu_2 = \frac{c_v}{\sqrt{mk_1}}; \lambda = \frac{k_3 v_{st}^2}{k_1}; \omega_1^2 = 1 + \lambda; \omega_2^2 = 1 + 3\lambda; f = \frac{e_d}{v_{st}}; \Omega^2 = \frac{m\omega^2}{k_1} \tag{12}$$

From Equations (10) and (11), we remark that the linear natural frequencies of the horizontal and vertical directions are slightly different due to the nonlinearity of the restoring force and the static deflection  $v_{st}$  given by Equation (5). Furthermore, the same effects produce an asymmetric nonlinear quadratic component.

In what follows, an approximate analytical solution will be determined to the asymmetric system (10) and (11) using the Optimal Auxiliary Functions Method (OAFM).

### 3. Basics of the OAFM

The nonlinear differential Equations (10) and (11) can be written in a general form as [22–27]:

$$L[X(\tau)] + N[X(\tau)] = 0 \tag{13}$$

where  $L$  is a linear operator,  $N$  is a nonlinear operator, and  $X(\tau)$  is an unknown function. In our particular case,  $X(\tau) = (u(\tau), v(\tau))$ . The corresponding boundary/initial conditions for Equation (13) are:

$$B(X(\tau), X'(\tau)) = 0 \tag{14}$$

We suppose that the approximate analytical solution  $\bar{X}(\tau)$  of Equation (13) can be rewritten in the form:

$$\bar{X}(\tau) = X_0(\tau) + X_1(\tau) \tag{15}$$

where the initial approximation  $X_0(\tau)$  and the first approximation  $X_1(\tau)$  can be determined as follows. Inserting Equation (15) into Equation (13) we are led to:

$$L[X_0(\tau)] + L[X_1(\tau)] + N[X_0(\tau) + X_1(\tau)] = 0 \tag{16}$$

The initial approximation  $X_0(\tau)$  is obtained by solving the linear differential equation:

$$L[X_0(\tau)] = 0, B\left[X_0(\tau), \frac{dX_0(\tau)}{d\tau}\right] = 0 \quad (17)$$

and the first approximation  $X_1(\tau)$  follows to be determined from the nonlinear equation:

$$L[X_1(\tau)] + N[X_0(\tau) + X_1(\tau)] = 0, B\left[X_1(\tau), \frac{dX_1(\tau)}{d\tau}\right] = 0 \quad (18)$$

The nonlinear operator  $N$  is expanded in the form:

$$N[X_0(\tau) + X_1(\tau)] = N[X_0(\tau)] + \sum_{k \geq 1} \frac{X_1^k(\tau)}{k!} N^{(k)}[X_0(\tau)] \quad (19)$$

To avoid the difficulties which appear when solving Equation (18), accelerating the convergence of the approximate solutions needs, instead of the last term from Equation (18), the employment of another expression. As such, Equation (18) can be rewritten:

$$L[X_1(\tau)] = \sum_{i=1}^p C_i F_i(\tau), B\left[X_1(\tau), \frac{dX_1(\tau)}{d\tau}\right] = 0 \quad (20)$$

where  $F_i(\tau)$ ,  $i = 1, 2, \dots, p$  and  $p$  are known auxiliary functions depending on the initial approximation  $X_0(\tau)$ , on the functions which appear in the composition of  $N[X_0(\tau)]$ , or the combination of such expressions. We remark that the  $p$  and the auxiliary functions  $F_i(\tau)$  are not unique. Accordingly,  $X_0(\tau)$  and  $N[X_0(\tau)]$  are sources for the auxiliary functions, and it should be emphasized that we have a large amount of freedom to choose these auxiliary functions. In expression (20),  $C_i$ ,  $i = 1, 2, \dots, p$  and  $p$  are unknown parameters at this moment. We remark that the nonlinear differential Equation (13) is reduced to only two linear differential Equations, namely (17) and (20).

Now, using the results obtained from the theory of differential equations, the variation of parameters method, Cauchy method, Kantorovich method, or the integral factor method [28], we have the freedom to choose the first approximation in the form:

$$X_1(\tau) = \sum_{i=1}^n f_i(F_j(\tau, C_j)) \quad (21)$$

where  $F_j$  are the auxiliary functions defined in Equation (20) and  $f_i$  are  $n$  functions depending on the functions  $F_j$ , satisfying the boundary/initial conditions:

$$B\left[f_i(F_j), \frac{\partial f_i(F_j)}{\partial \tau}\right] = 0, i = 1, 2, \dots, n \quad (22)$$

As a consequence, the first approximation  $X_1$  can be determined from Equations (21) and (22). Finally, the unknown parameters  $C_i$  are optimally identified via rigorous mathematical approaches, such as the collocation method, Galerkin method, Ritz method, the least square method, or by minimizing the residual error. In this way, the approximate solution  $\bar{X}(\tau)$  is well determined after the identification of the optimal values of the initially unknown convergence-control parameters  $C_i$ ,  $i = 1, 2, \dots, n$ .

We will prove that our approach is a very powerful tool for solving nonlinear problems without the presence of small or large parameters in the initial Equation (13) or the boundary/initial conditions (14).

#### 4. Application of OAFM to Nonlinear Oscillations of Jeffcott Rotor

We will use the basic ideas of the OAFM, considering Equations (20) and (21) with the initial conditions:

$$u(0) = A, v(0) = B, u'(0) = 0, v'(0) = 0 \tag{23}$$

By setting:

$$u(\tau) = Ax(\tau), v(\tau) = By(\tau) \tag{24}$$

the initial conditions (23) can be rewritten as:

$$x(0) = 1, y(0) = 1, x'(0) = 0, y'(0) = 0, \tag{25}$$

inserting Equation (24) into Equations (10) and (11) yields:

$$x'' + 2\mu_1x' + \omega_1^2x + 2\lambda Bxy + \lambda(A^2x^3 + B^2xy^2) - \frac{f}{A}\Omega^2 \cos \Omega\tau = 0, \tag{26}$$

$$y'' + 2\mu_2y' + \omega_2^2y + \lambda(\frac{A^2}{B}x^2 + 3By^2) + \lambda(A^2x^2y + B^2y^3) - \frac{f}{B}\Omega^2 \sin \Omega\tau = 0 \tag{27}$$

The linear and nonlinear operators for the last equations are respectively:

$$L[x(\tau)] = x'' + 2\mu_1x' + \omega_1^2x; L[y(\tau)] = y'' + 2\mu_2y' + \omega_2^2y, \tag{28}$$

$$N_1(x, y) = 2\lambda Bxy + \lambda(A^2x^3 + B^2xy^2) - \frac{f}{A}\Omega^2 \cos \Omega\tau, \tag{29}$$

$$N_2(x, y) = \lambda(\frac{A^2}{B}x^2 + 3By^2) + \lambda(A^2x^2y + B^2y^3) - \frac{f}{B}\Omega^2 \sin \Omega\tau, \tag{30}$$

In accordance with the OAFM algorithm, the approximate solution of Equations (26) and (27) is:

$$\bar{X}(\tau) = x_0(\tau) + x_1(\tau); \bar{y}(\tau) = y_0(\tau) + y_1(\tau), \tag{31}$$

The initial approximations can be determined from Equations (17) and (28):

$$x''_0 + 2\mu_1x'_0 + \omega_1^2x_0 = 0, x_0(0) = 1, x'_0(0) = 0, \tag{32}$$

$$y''_0 + 2\mu_2y'_0 + \omega_2^2y_0 = 0, y_0(0) = 1, y'_0(0) = 0, \tag{33}$$

The above equations have the solutions:

$$x_0(\tau) = e^{-\mu_1\tau} \left( \cos p_1\tau + \frac{\mu_1}{p_1} \sin p_1\tau \right), \tag{34}$$

$$y_0(\tau) = e^{-\mu_2\tau} \left( \cos p_2\tau + \frac{\mu_2}{p_2} \sin p_2\tau \right), \tag{35}$$

where:

$$p_1^2 = \omega_1^2 - \mu_1^2, p_2^2 = \omega_2^2 - \mu_2^2. \tag{36}$$

Inserting Equation (34) into Equation (29) and then Equation (35) into Equation (30), we obtain:

$$\begin{aligned} N_1(x_0, y_0) = & M_1e^{-3\mu_1\tau} \cos p_1\tau + M_2e^{-3\mu_1\tau} \sin p_1\tau + M_3e^{-(\mu_1+2\mu_2)\tau} \sin p_1\tau + \\ & + M_4e^{-3\mu_1\tau} \cos 3p_1\tau + M_5e^{-3\mu_1\tau} \sin 3p_1\tau + M_6e^{-(\mu_1+\mu_2)\tau} [\cos(p_1 + p_2)\tau + \\ & + \cos(p_1 - p_2)\tau] + M_7e^{-(\mu_1+\mu_2)\tau} \sin(p_1 + p_2)\tau + M_8e^{-(\mu_1+\mu_2)\tau} \sin(p_1 - p_2)\tau + \\ & + M_9e^{-(\mu_1+2\mu_2)\tau} [\cos(2p_2 - p_1)\tau - \cos(2p_2 + p_1)\tau] + \\ & + M_{10}e^{-(\mu_1+2\mu_2)\tau} [\sin(p_1 + 2p_2)\tau + \sin(p_1 - 2p_2)\tau] - \frac{f}{A}\Omega^2 \cos \Omega\tau \end{aligned} \tag{37}$$

$$\begin{aligned}
 N_2(x_0, y_0) = & Q_1 e^{-(2\mu_1 + \mu_2)\tau} \cos p_2 \tau + Q_2 e^{-(2\mu_1 + \mu_2)\tau} \sin p_2 \tau + Q_3 e^{-(2\mu_1 + \mu_2)\tau} \cos(2p_1 - p_2)\tau + \\
 & + Q_4 e^{-(2\mu_1 + \mu_2)\tau} \sin(2p_1 - p_2)\tau + Q_5 e^{-(2\mu_1 + \mu_2)\tau} \cos(2p_1 - p_2)\tau + Q_6 e^{-(2\mu_1 + \mu_2)\tau} \sin(2p_1 + p_2)\tau + \\
 & + Q_7 e^{-3\mu_2\tau} \cos 3p_2 \tau + Q_8 e^{-3\mu_2\tau} \sin 3p_2 \tau + Q_9 e^{-2\mu_2\tau} \cos 2p_1 \tau + \\
 & + Q_{10} e^{-2\mu_1\tau} \sin p_1 \tau + Q_{11} e^{-2\mu_1\tau} + Q_{12} e^{-2\mu_2\tau} \cos 2p_2 \tau + Q_{13} e^{-2\mu_2\tau} \sin 2p_2 \tau + Q_{14}
 \end{aligned}
 \tag{38}$$

where the values of the parameters  $M_i$  and  $Q_i$  are given in the Appendix A.

In the study we will consider two possible cases:

- (1) Simultaneous resonance  $\Omega = \omega_1 \approx \omega_2$ ;
- (2) Internal resonance  $\omega_1 \approx \omega_2, \Omega \neq \omega_1$ .

4.1. Application of OAFM to Nonlinear Oscillations of Jeffcott Rotor in the Case of Simultaneous Resonance

In this subcase from Equation (37), the auxiliary functions can be chosen as:

$$\begin{aligned}
 F_1(\tau) = e^{-\mu_1\tau}; F_2(\tau) = e^{-\mu_1\tau} \sin \Omega\tau, F_3(\tau) = e^{-2\mu_1\tau} \cos \Omega\tau; \\
 F_4(\tau) = e^{-2\mu_1\tau} \sin \Omega\tau; F_5(\tau) = e^{-3\mu_1\tau} \cos \Omega\tau; F_6(\tau) = e^{-3\mu_1\tau} \sin \Omega\tau
 \end{aligned}
 \tag{39}$$

or:

$$\begin{aligned}
 F_1(\tau) = e^{-\mu_1\tau} \cos 2\Omega\tau; F_2(\tau) = e^{-\mu_1\tau} \sin 2\Omega\tau, F_3(\tau) = e^{-2\mu_1\tau} \cos 3\Omega\tau; \\
 F_4(\tau) = e^{-3\mu_1\tau} \sin 3\Omega\tau F_5(\tau) = e^{-4\mu_1\tau} \cos 4\Omega\tau; F_6(\tau) = e^{-4\mu_1\tau} \sin 4\Omega\tau
 \end{aligned}
 \tag{40}$$

or even:

$$\begin{aligned}
 f_1(\tau) = (e^{-\mu_1\tau} - e^{-2\mu_1\tau}) \cos \Omega\tau - \frac{\mu_1}{\Omega} e^{-\mu_1\tau} \sin \Omega\tau, f_2(\tau) = (e^{-\mu_1\tau} - e^{-3\mu_1\tau}) \cos \Omega\tau \\
 - \frac{2\mu_1}{\Omega} e^{-\mu_1\tau} \sin \Omega\tau, f_3(\tau) = (e^{-\mu_1\tau} - e^{-4\mu_1\tau}) \cos \Omega\tau - \frac{3\mu_1}{\Omega} e^{-\mu_1\tau} \sin \Omega\tau
 \end{aligned}
 \tag{41}$$

and so on.

Considering only the auxiliary functions (39) from Equations (21) and (22), we can choose the functions  $f_i$ , such as  $f_i(0) = f'_i(0) = 0$ . It follows that:

$$\begin{aligned}
 f_1(\tau) = (e^{-\mu_1\tau} - e^{-2\mu_1\tau}) \cos \Omega\tau - \frac{\mu_1}{\Omega} e^{-\mu_1\tau} \sin \Omega\tau, f_2(\tau) = (e^{-\mu_1\tau} - e^{-3\mu_1\tau}) \cos \Omega\tau - \\
 - \frac{2\mu_1}{\Omega} e^{-\mu_1\tau} \sin \Omega\tau, f_3(\tau) = (e^{-\mu_1\tau} - e^{-4\mu_1\tau}) \cos \Omega\tau - \frac{3\mu_1}{\Omega} e^{-\mu_1\tau} \sin \Omega\tau
 \end{aligned}
 \tag{42}$$

The first approximation (21) for Equation (26) becomes:

$$x_1(\tau) = C_1 f_1(\tau) + C_2 f_2(\tau) + C_3 f_3(\tau)
 \tag{43}$$

The auxiliary functions from Equation (27) can be chosen in the same manner as for Equation (37), and it follows that:

$$\begin{aligned}
 g_1(\tau) = (e^{-\mu_2\tau} - e^{-2\mu_2\tau}) \cos \Omega\tau - \frac{\mu_2}{\Omega} e^{-\mu_2\tau} \sin \Omega\tau, g_2(\tau) = (e^{-\mu_2\tau} - e^{-3\mu_2\tau}) \cos \Omega\tau - \\
 - \frac{2\mu_2}{\Omega} e^{-\mu_2\tau} \sin \Omega\tau, g_3(\tau) = (e^{-\mu_2\tau} - e^{-4\mu_2\tau}) \cos \Omega\tau - \frac{3\mu_2}{\Omega} e^{-\mu_2\tau} \sin \Omega\tau
 \end{aligned}
 \tag{44}$$

The first approximation (21) for Equation (27) is:

$$y_1(\tau) = C_4 g_1(\tau) + C_5 g_2(\tau) + C_6 g_3(\tau)
 \tag{45}$$

where  $C_i, i = 1, 2, \dots, 6$  are unknown parameters at this moment.

The approximate solutions for Equations (26) and (27) are obtained from Equations (31), (34), (35), (43), and (45) as:

$$\begin{aligned}
 \bar{x}(\tau) = e^{-\mu_1\tau} (\cos \Omega\tau + \frac{\mu_1}{\Omega} \sin \Omega\tau) + C_1 [(e^{-\mu_1\tau} - e^{-2\mu_1\tau}) \cos \Omega\tau - \frac{\mu_1}{\Omega} e^{-\mu_1\tau} \sin \Omega\tau] + \\
 + C_2 [(e^{-\mu_1\tau} - e^{-3\mu_1\tau}) \cos \Omega\tau - \frac{2\mu_1}{\Omega} e^{-\mu_1\tau} \sin \Omega\tau] + C_3 [(e^{-\mu_1\tau} - e^{-4\mu_1\tau}) \cos \Omega\tau - \frac{3\mu_1}{\Omega} e^{-\mu_1\tau} \sin \Omega\tau]
 \end{aligned}
 \tag{46}$$

$$\begin{aligned}
 \bar{y}(\tau) = e^{-\mu_2\tau} (\cos \Omega\tau + \frac{\mu_2}{\Omega} \sin \Omega\tau) + C_4 [(e^{-\mu_2\tau} - e^{-2\mu_2\tau}) \cos \Omega\tau - \frac{\mu_2}{\Omega} e^{-\mu_2\tau} \sin \Omega\tau] + \\
 + C_5 [(e^{-\mu_2\tau} - e^{-3\mu_2\tau}) \cos \Omega\tau - \frac{2\mu_2}{\Omega} e^{-\mu_2\tau} \sin \Omega\tau] + C_6 [(e^{-\mu_2\tau} - e^{-4\mu_2\tau}) \cos \Omega\tau - \frac{3\mu_2}{\Omega} e^{-\mu_2\tau} \sin \Omega\tau]
 \end{aligned}
 \tag{47}$$

4.2. Application of OAFM to Nonlinear Oscillations of Jeffcott Rotor in the Case of Internal Resonance

Taking into account that  $\Omega \neq \omega_1 \approx \omega_2$ , the functions  $f_i$  from Equation (42) and  $g_i$  from Equation (44) will depend on the  $p_1, p_2$ , and  $\Omega$ , as follows:

$$f_1(\tau) = (e^{-\mu_1\tau} - e^{-2\mu_1\tau}) \cos p_1\tau - \frac{\mu_1}{p_1} e^{-\mu_1\tau} \sin p_1\tau, f_2(\tau) = (e^{-\mu_1\tau} - e^{-3\mu_1\tau}) \cos p_1\tau - \frac{2\mu_1}{p_1} e^{-\mu_1\tau} \sin p_1\tau, f_3(\tau) = (e^{-\mu_1\tau} - e^{-2\mu_1\tau}) \cos \Omega\tau - \frac{\mu_1}{\Omega} \sin \Omega\tau \tag{48}$$

$$g_1(\tau) = (e^{-\mu_2\tau} - e^{-2\mu_2\tau}) \cos p_2\tau - \frac{\mu_2}{p_2} e^{-\mu_2\tau} \sin p_2\tau, g_2(\tau) = (e^{-\mu_2\tau} - e^{-3\mu_2\tau}) \cos p_2\tau - \frac{2\mu_2}{p_2} e^{-\mu_2\tau} \sin p_2\tau, g_3(\tau) = (e^{-\mu_2\tau} - e^{-3\mu_2\tau}) \cos \Omega\tau - \frac{2\mu_2}{\Omega} \sin \Omega\tau \tag{49}$$

so that the approximate analytical solution for Equations (26) and (27) obtained from Equations (31), (34), (35), (48), and (49) are:

$$\bar{x}(\tau) = e^{-\mu_1\tau} (\cos p_1\tau - \frac{\mu_1}{p_1} \sin p_1\tau) + C_7 f_1(\tau) + C_8 f_2(\tau) + C_9 f_3(\tau) \tag{50}$$

$$\bar{y}(\tau) = e^{-\mu_2\tau} (\cos p_2\tau - \frac{\mu_2}{p_2} \sin p_2\tau) + C_{10} g_1(\tau) + C_{11} g_2(\tau) + C_{12} g_3(\tau) \tag{51}$$

where  $C_i, i = 7, 8, \dots, 12$  are unknown parameters and  $f_i, g_i$  are given by Equations (48) and (49), respectively.

5. Numerical Example

In order to prove the accuracy of our approach, we consider that the data for Equations (25)–(27) for every case (simultaneous resonance and internal resonance) are as follows:

5.1. The Case of Simultaneous Resonance

For the simultaneous resonance ( $\Omega = \omega_1 = \omega_2$ ), the parameters are:

$$\mu_1 = 0.0077, \mu_2 = 0.10735, \lambda = 0.01, \Omega = \omega_1 = 1.004987, \omega_2 = 1.01489, f = 0.025, A = 1, B = 2 \tag{52}$$

The optimal values of the convergence-control parameters  $C_i, i = 1, 2, \dots, 6$  are obtained by means of a collocation approach [23], such as:

$$C_1 = -2.417585842221364, C_2 = 1.3698671035721188, C_3 = 0.0113075348472 \tag{53}$$

$$C_4 = -0.9146640575257668, C_5 = 0.5504407549657382, C_6 = 0.0210144382104 \tag{54}$$

The approximate solutions of Equations (10), (11), and (13) in the case of the simultaneous resonance are:

$$\bar{u}(\tau) = e^{-\mu_1\tau} (\cos \Omega\tau + \frac{\mu_1}{\Omega} \sin \Omega\tau) - 2.417585842221364 [(e^{-\mu_1\tau} - e^{-2\mu_1\tau}) \cos \Omega\tau - \frac{\mu_1}{\Omega} e^{-\mu_1\tau} \sin \Omega\tau] + 1.3698671035721188 [(e^{-\mu_1\tau} - e^{-3\mu_1\tau}) \cos \Omega\tau - \frac{2\mu_1}{\Omega} e^{-\mu_1\tau} \sin \Omega\tau] + 0.0113075348472 [(e^{-\mu_1\tau} - e^{-4\mu_1\tau}) \cos \Omega\tau - \frac{3\mu_1}{\Omega} e^{-\mu_1\tau} \sin \Omega\tau] \tag{55}$$

$$\bar{v}(\tau) = 2e^{-\mu_2\tau} (\cos \Omega\tau + \frac{\mu_2}{\Omega} \sin \Omega\tau) - 0.9146640575257668 [(e^{-\mu_2\tau} - e^{-2\mu_2\tau}) \cos \Omega\tau - \frac{\mu_2}{\Omega} e^{-\mu_2\tau} \sin \Omega\tau] + 0.5504407549657382 [(e^{-\mu_2\tau} - e^{-3\mu_2\tau}) \cos \Omega\tau - \frac{2\mu_2}{\Omega} e^{-\mu_2\tau} \sin \Omega\tau] + 0.0210144382104 [(e^{-\mu_2\tau} - e^{-4\mu_2\tau}) \cos \Omega\tau - \frac{3\mu_2}{\Omega} e^{-\mu_2\tau} \sin \Omega\tau] \tag{56}$$

In Figures 2 and 3, the approximate analytical solutions,  $\bar{u}$  and  $\bar{v}$ , are graphically presented, as given by Equations (55) and (56), in comparison with the corresponding numerical integration results obtained from Equations (10), (11), (23), and (52) in the case of simultaneous resonance.

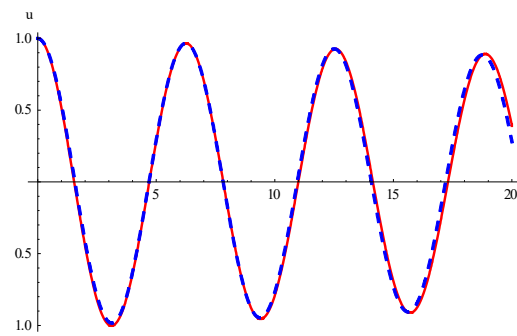


**Figure 2.** Comparison between the numerical solution of Equations (10) and (23) at simultaneous resonance and approximate solution (55): — numerical integration solution; - - - analytical solution.

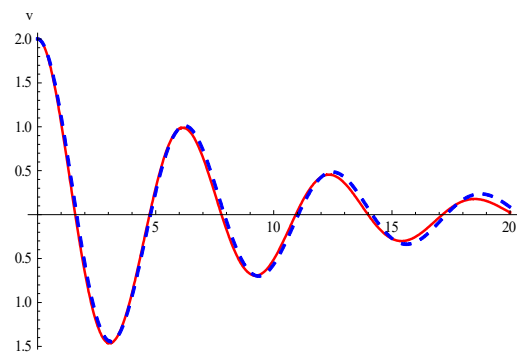


**Figure 3.** Comparison between the numerical solution of Equations (11) and (23) at simultaneous resonance and approximate solution (56): — numerical integration solution; - - - analytical solution.

### 5.2. The Case of Internal Resonance

In the case of internal resonance, the parameters are chosen as:

$$\begin{aligned} \mu_1 &= 0.0077, \mu_2 = 0.10735, \lambda = 0.01, \Omega = 0.5, \omega_1 = 1.0049 \\ \omega_2 &= 1.01489, f = 0.025, A = B = 1, p_1 = 1.004958; p_2 = 1.00919 \end{aligned} \quad (57)$$

The optimal values of the convergence-control parameters in this case are:

$$C_7 = -0.402383803986711, C_8 = 0.174367028869554, C_9 = 0.172699630062805 \quad (58)$$

$$C_{10} = -0.002619502362916, C_{11} = 0.007970571212564, C_{12} = -0.005892786988971 \quad (59)$$

The approximate solution in the case of the internal resonance of Equations (10), (11), and (23) becomes:

$$\begin{aligned} \bar{u}(\tau) &= e^{-\mu_1 \tau} (\cos p_1 \tau + \frac{\mu_1}{p_1} \sin p_1 \tau) - 0.402383803986711 [(e^{-\mu_1 \tau} - e^{-2\mu_1 \tau}) \cos p_1 \tau - \frac{\mu_1}{p_1} e^{-\mu_1 \tau} \sin p_1 \tau] + \\ &+ 0.174367028869554 [(e^{-\mu_1 \tau} - e^{-3\mu_1 \tau}) \cos p_1 \tau - \frac{2\mu_1}{p_1} e^{-\mu_1 \tau} \sin p_1 \tau] + \\ &+ 0.172699630062805 [(e^{-\mu_1 \tau} - e^{-4\mu_1 \tau}) \cos \Omega \tau - \frac{3\mu_1}{\Omega} e^{-\mu_1 \tau} \sin \Omega \tau] \end{aligned} \quad (60)$$

$$\begin{aligned} \bar{v}(\tau) &= e^{-\mu_2 \tau} (\cos p_2 \tau + \frac{\mu_2}{p_2} \sin p_2 \tau) - 0.002619502362916 [(e^{-\mu_2 \tau} - e^{-2\mu_2 \tau}) \cos p_2 \tau - \\ &- \frac{\mu_2}{p_2} e^{-\mu_2 \tau} \sin p_2 \tau] + 0.007970571212564 [(e^{-\mu_2 \tau} - e^{-3\mu_2 \tau}) \cos p_2 \tau - \frac{2\mu_2}{p_2} e^{-\mu_2 \tau} \sin p_2 \tau] + \\ &- 0.005892786988971 [(e^{-\mu_2 \tau} - e^{-3\mu_2 \tau}) \cos \Omega \tau - \frac{2\mu_2}{\Omega} e^{-\mu_2 \tau} \sin \Omega \tau] \end{aligned} \quad (61)$$

In Figures 4 and 5, we compared the numerical solutions of Equations (10) and (11), and the approximate solutions (60) and (61), respectively, for the case of internal resonance.

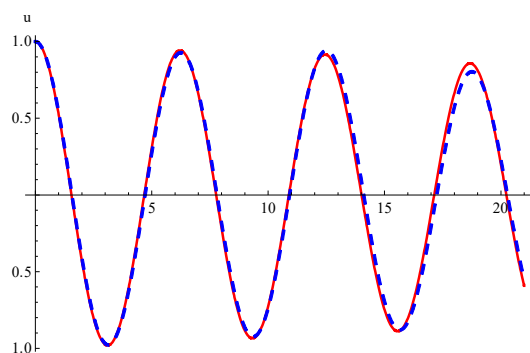


**Figure 4.** Comparison between the numerical solution of Equations (10) and (23) at internal resonance and approximate solution (60): — numerical integration solution; - - - analytical solution..

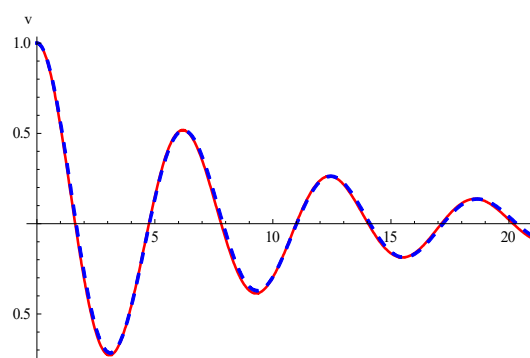


**Figure 5.** Comparison between the numerical solution of Equations (11) and (23) at internal resonance and approximate solution (61): — numerical integration solution; - - - analytical solution.

From Figures 2–5, a very good agreement can be observed between the approximate solutions and numerical integration results, which confirms the great potential of the OAFM.

## 6. Conclusions

The objective of this research is the study of the nonlinear vibration of a horizontally supported Jeffcott rotor with quadratic and cubic nonlinearity, where the nonlinear restoring force, due to the bearing clearance and the rotor weight, is considered. The linear natural frequencies in the horizontal and vertical directions have small differences due to the nonlinearity of the restoring force and disk weight.

The nonlinear vibrations of the horizontally supported Jeffcott rotor are generated by the rotor eccentricity.

Explicit analytical solutions for the two cases are established using our original Optimal Auxiliary Functions Method (OAFM). Our approach considerably simplifies calculations because any nonlinear differential equation is reduced to two linear ordinary differential equations using the so-called auxiliary functions. This idea does not appear in any other methods known in the scientific literature. Our technique is different from other traditional procedures, especially concerning the optimal auxiliary functions that depend on some initially unknown parameters. We have a large degree of freedom to choose the auxiliary functions and the number of convergence-control parameters.

The obtained approximate analytical solutions are in excellent agreement with the numerical integration results in all cases. Our technique is valid, even if the nonlinear governing equations do not contain small or large parameters. The construction of the first iterations is completely different from other known methods. The optimal values of the convergence-control parameters are identified by means of a rigorous mathematical procedure, providing a fast convergence of the approximate analytical solutions using only the first iteration.

It is proved that the OAFM is very effective and efficient in practice. This research provides helpful guidance to solve dynamic problems, and may help to design and manufacture more reliable engineering products.

**Author Contributions:** Conceptualization, V.M. and N.H.; methodology, V.M. and N.H.; software, N.H.; validation, V.M. and N.H.; formal analysis, V.M.; investigation, V.M. and N.H.; resources, N.H.; data curation, V.M. and N.H.; writing—original draft preparation, V.M. and N.H.; writing—review and editing, V.M. and N.H.; visualization, N.H.; supervision, N.H.; project administration, V.M. and N.H.; funding acquisition, N.H. All authors have read and agreed to the published version of the manuscript.

**Funding:** This research received no external funding.

**Institutional Review Board Statement:** Not applicable.

**Informed Consent Statement:** Not applicable.

**Data Availability Statement:** All data are presented within the paper.

**Acknowledgments:** The authors would like to thank the reviewers for their valuable comments and helpful suggestions.

**Conflicts of Interest:** The authors declare no conflict of interest.

## Appendix A

$$\begin{aligned}
 M_1 &= \frac{\lambda A^2}{4} \left( 3 + \frac{\mu_1^2}{p_1^2} \right); M_2 = \frac{\lambda A^2}{4} \frac{\mu_1}{p_1} \left( 5 + \frac{3\mu_1^2}{p_1^2} \right); M_3 = \frac{\lambda B^2}{2} \frac{\mu_1}{p_1} \left( 1 + \frac{3\mu_2^2}{p_2^2} \right) \\
 M_4 &= \frac{\lambda A^2}{4} \left( 1 - \frac{5\mu_1^2}{p_1^2} \right); M_5 = \frac{\lambda A^2}{4} \frac{\mu_1}{p_1} \left( 5 - \frac{\mu_1^2}{p_1^2} \right); M_6 = \lambda B^2 \left( 1 + \frac{\mu_1 \mu_2}{p_1 p_2} \right) \\
 M_7 &= \lambda B \left( \frac{\mu_1}{p_1} + \frac{\mu_2}{p_2} \right); M_8 = \lambda B \left( \frac{\mu_1}{p_1} - \frac{\mu_2}{p_2} \right); M_9 = \lambda B^2 \frac{\mu_1 \mu_2}{p_1 p_2}; M_{10} = \frac{\lambda B^2}{4} \frac{\mu_1}{p_1} \left( 1 - \frac{\mu_2^2}{p_2^2} \right) \\
 Q_1 &= \frac{\lambda A^2}{2} \left( 1 + \frac{\mu_1^2}{p_1^2} \right); Q_2 = \frac{\lambda A^2}{2} \frac{\mu_2}{p_2} \left( 1 + \frac{\mu_2}{p_2} \right); Q_3 = \lambda A^2 \left( \frac{1}{4} + \frac{\mu_1 \mu_2}{p_1 p_2} - \frac{\mu_1^2}{4p_1^2} \right) \\
 Q_4 &= \lambda A^2 \left( \frac{\mu_1}{p_1} - \frac{\mu_2}{4p_2} + \frac{\mu_1^2 \mu_2}{4p_1^2 p_2} \right); Q_5 = \lambda A^2 \left( \frac{1}{4} - \frac{\mu_1 \mu_2}{p_1 p_2} - \frac{\mu_1^2}{4p_1^2} \right); Q_6 = \lambda A^2 \left( \frac{\mu_1}{p_1} + \frac{\mu_2}{4p_2} - \frac{\mu_1^2 \mu_2}{4p_1^2 p_2} \right) \\
 Q_7 &= \frac{\lambda B^2}{2} \left( 3 - \frac{5\mu_2^2}{p_2^2} \right); Q_8 = \frac{\lambda B^2}{2} \frac{\mu_2}{p_2} \left( 5 - \frac{3\mu_2^2}{p_2^2} \right); Q_9 = \frac{\lambda A^2}{2B} \left( 1 - \frac{\mu_1^2}{2p_1^2} \right); Q_{10} = \frac{2\lambda A^2}{B} \frac{\mu_1}{p_1} \\
 Q_{11} &= \frac{\lambda A^2}{2B}; Q_{12} = \frac{3\lambda B}{2} \left( 1 - \frac{\mu_2^2}{p_2^2} \right); Q_{13} = 3\lambda B \frac{\mu_2}{p_2}; Q_{14} = \frac{3\lambda B}{2} \left( 1 + \frac{\mu_2^2}{2p_2^2} \right)
 \end{aligned}$$

## References

- Keogh, P.S. Contact dynamics phenomena in rotating machines active/passive consideration. *Mech. Syst. Signal Proc.* **2012**, *29*, 19–33. [\[CrossRef\]](#)
- Muszinska, A. Synchronous self-excited rotor vibration caused by a full annular rub. In *Machinery Dynamics 8th Seminar*; Canadian Machinery Association: Halifax, NS, Canada, 1984; pp. 22.1–22.21.
- Karlberg, M.; Aidanpaa, J.-O. Numerical investigation of an unbalance rotor system with bearing clearance. *Chaos Solitons Fractals* **2003**, *18*, 653–664. [\[CrossRef\]](#)
- Patel, T.H.; Darpe, A.K. Study of coast-up vibration response for rub detection. *Mech. Mach. Theory* **2009**, *44*, 1570–1579. [\[CrossRef\]](#)
- Khanlo, H.M.; Ghayour, M.; Rad, S.Z. Chaotic vibration analysis of rotation, flexible, continuous shaft-disk system with a rub-impact between the disk and the rotor. *Commun. Nonlin. Sci. Numer. Simul.* **2011**, *16*, 566–581. [\[CrossRef\]](#)
- Yabuno, H.; Kashimura, T.; Inoue, T.; Ishida, Y. Nonlinear normal modes and primary resonance of horizontally supported Jeffcott rotor. *Nonlin. Dyn.* **2011**, *66*, 377–387.
- Lahriri, S.; Weber, H.I.; Santos, I.F.; Hartmann, H. Rotor-stator contact dynamics using a non-ideal drive. Theoretical and experimental aspects. *J. Sound. Vibr.* **2012**, *331*, 4518–4536. [\[CrossRef\]](#)
- Dimarogonas, A.D.; Paipetis, S.A.; Chondros, T.G. *Analytical Methods in Rotor Dynamics*, 2nd ed.; Springer: London, UK, 2013.
- Chavez, J.P.; Wiercigroch, M. Bifurcation analysis of periodic orbits of a smooth Jeffcott rotor model. *Commun. Nonlin. Sci. Numer. Simul.* **2013**, *18*, 2571–2580. [\[CrossRef\]](#)
- Gu, L.; Chu, F. An analytical study of rotor dynamics coupled with thermal effect for a continuous rotor shaft. *J. Sound. Vibr.* **2014**, *333*, 4030–4050. [\[CrossRef\]](#)
- Hou, J.; Chen, Y.; Cao, Q. Nonlinear vibration phenomenon of an aircraft rub-impact rotor system due to hovering flight. *Commun. Nonlin. Sci. Numer. Simul.* **2014**, *19*, 286–297. [\[CrossRef\]](#)
- Ma, H.; Lu, Y.; Wu, Z.; Tai, X.; Li, H.; Wen, B. A new dynamic model of rotor-blade systems. *J. Sound. Vibr.* **2015**, *357*, 168–184. [\[CrossRef\]](#)

13. Yang, Y.; Wang, Y.; Gao, Z. Nonlinear analysis of a rub-impact rotor with random stiffness under random excitation. *Adv. Mech. Eng.* **2016**, *8*, 1687814016668090. [[CrossRef](#)]
14. Bergeot, B.; Bellizi, S.; Cochelin, B. Passive suppression of helicopter ground resonance using nonlinear energy sinks attached on the helicopter blades. *J. Sound. Vibr.* **2017**, *392*, 41–55. [[CrossRef](#)]
15. Saeed, N.A.; El-Gohary, H.A. On the nonlinear oscillations of a horizontally supported Jeffcott rotor with a nonlinear restoring force. *Nonlin. Dyn.* **2017**, *88*, 293–314. [[CrossRef](#)]
16. Hang, J.; Yu, P.; Zhang, D.; Ma, Y. Nonlinear dynamic analysis using the complex nonlinear modes for a rotor system with an additional constraint due to rub-impact. *Mech. Syst. Signal Proc.* **2018**, *118*, 443–461. [[CrossRef](#)]
17. Eftekhari, M.; Rahmatabadi, A.D.; Mazidi, A. Magnetic field effect on the nonlinear vibration of a rotor. *Appl. Math. Mech. Engl. Ed.* **2020**, *41*, 289–312. [[CrossRef](#)]
18. Li, S.; Liu, F.; Wang, H.; Song, H.; Yu, K. Nonlinear vibration analysis of rotor considering cogging and harmonic effects. *Shock Vibr.* **2021**, *2021*, 6685588. [[CrossRef](#)]
19. Tchameni, B.K.; Alugongo, A. Vibration of misaligned rotor system with hysteretic friction arising from driveshaft contact under dispersed viscous fluid influences. *Appl. Sci.* **2021**, *11*, 8089. [[CrossRef](#)]
20. Jin, Y.; Liu, Z.; Yang, Y.; Li, F.; Chen, Y. Nonlinear vibrations of a dual rotor bearing coupling misalignment system with blade-casing rubbing. *J. Sound. Vibr.* **2021**, *497*, 115948. [[CrossRef](#)]
21. Saeed, N.A.; Awwad, E.M.; Maarouf, A.; Farh, H.M.N.; Alurki, F.A.; Awrejcewicz, J. Rub-impact force induces periodic, quasiperiodic, and chaotic motions of a controlled asymmetric rotor system. *Shock Vibr.* **2021**, *2021*, 1800022. [[CrossRef](#)]
22. Marinca, V.; Herisanu, N.; Marinca, B. *Optimal Auxiliary Functions Method for Nonlinear Dynamical Systems*; Springer: Cham, Switzerland, 2021.
23. Herisanu, N.; Marinca, V. A solution procedure combining analytical and numerical approaches to investigate a two-degree of freedom vibro-impact oscillator. *Mathematics* **2021**, *9*, 1374. [[CrossRef](#)]
24. Marinca, B.; Marinca, V.; Bogdan, C. Dynamics of SEIR epidemic model by Optimal Auxiliary Functions Method. *Chaos Solitons Fractals* **2021**, *147*, 110949. [[CrossRef](#)] [[PubMed](#)]
25. Herisanu, N.; Marinca, V.; Madescu, G.; Dragan, F. Dynamic response of a permanent magnet synchronous generator to a wind gust. *Energies* **2019**, *12*, 915. [[CrossRef](#)]
26. Herisanu, N.; Marinca, V. An efficient analytical approach to investigate the dynamics of a misaligned multirotor system. *Mathematics* **2020**, *8*, 1083. [[CrossRef](#)]
27. Marinca, V.; Herisanu, N. Construction of analytic solutions to axisymmetric flow and heat transfer on a moving cylinder. *Symmetry* **2020**, *12*, 1335. [[CrossRef](#)]
28. Elsgolts, L. *Differential Equations and Calculus of Variations*; Mir: Moscow, Russia, 1977.